\$ SUPER

Contents lists available at ScienceDirect

### **Immunobiology**

journal homepage: www.elsevier.com/locate/imbio



# Absence of complement terminal pathway activity in C6-deficient mice prolongs survival in a mouse model of severe malarial infection<sup>☆</sup>

Tomoaki Kamiya <sup>a</sup>, Yuki Miyasaka <sup>b</sup>, Hangsoo Kim <sup>a,c</sup>, Sosuke Fukui <sup>a,c</sup>, Masatoshi Inoue <sup>a</sup>, Masatoshi Ishigami <sup>d</sup>, Yasuhiro Suzuki <sup>a,c</sup>, Shoichi Maruyama <sup>a</sup>, Tamio Ohno <sup>b</sup>, Timothy R. Hughes <sup>e</sup>, B. Paul Morgan <sup>e</sup>, Masashi Mizuno <sup>a,c,\*</sup>

- <sup>a</sup> Department of Nephrology, Nagoya University Graduate School of Medicine, Nagaya, Japan
- <sup>b</sup> Division of Experimental Animals, Nagoya University Graduate School of Medicine, Nagaya, Japan
- <sup>c</sup> Department of Renal Replacement Therapy, Nagoya University Graduate School of Medicine, Nagaya, Japan
- <sup>d</sup> Department of Gastroenterology and Hepatology, Nagoya University Graduate School of Medicine, Nagaya, Japan
- <sup>e</sup> Division of Infection and Immunity, School of Medicine, Cardiff University, Cardiff, UK

#### ARTICLE INFO

#### Editor name: Viviana P. Ferreira

Keywords: Malaria Multiple organ failures Complement system Terminal pathway

Infection

#### ABSTRACT

Background: Malaria is an important and serious parasite-induced disease associated with severe anemia and multiple organ failure (MOF) that can be lethal in humans. We explored the contribution of the terminal pathway of complement in a mouse model of malaria-induced lethal MOF following infection with Plasmodium (P.) bergei. Methods: We compared organ damage and survival between C57BL/6 J mice deficient in the terminal pathway component C6 (C6def) and wild type C57BL/6 J mice (WT) after intraperitoneal injection of 10<sup>6</sup> P. bergei-parasitized erythrocytes. We measured survival, relevant blood parameters, assessed severity of injury and complement activation in relevant organs.

Results: All WT mice died between 7 and 13 days after exposure to the parasite challenge; in contrast, C6def mice showed prolonged survival with 80 % alive at day 20, although all then died by day 26. Parasite load and anemia at day 7 were similar in C6def and WT mice. Liver and lung injuries, fibrosis and organ complement deposition assessed at day 7 post-infection were significantly milder in C6def mice compared to WT. Blood platelet count at day 7 post-infection was markedly reduced in WT but not in C6def mice; in contrast, white cell count was increased and hemoglobin levels decreased to similar degrees in WT and C6def mice post-infection. Albumin levels were reduced, significantly more in WT, while blood markers of liver injury were increased, significantly more in WT. Serum levels of complement activation product, C5a, and IL6 were increased in both groups, the latter significantly higher in WT versus C6def mice.

Conclusion: We show that complement terminal pathway activation exacerbates organ injuries and thrombocy-topenia associated with *P. bergei* infection, contributing to rapid progression to death in the model. Inhibition of terminal pathway activation in human malarial infections using available drugs might slow progression to organ failure, extending the window of opportunity for the effective use of anti-malarial medicines.

#### 1. Introduction

Malaria is a consequence of infection by one of the five pathogenic *Plasmodium (P.) species (spp.), P. falciparum, P. vivax, P. ovale, P. malatia* or *P. knowlesi* (Biryukov and Stoute, 2014). The WHO World Malaria Report 2024 (https://www.who.int/teams/global-malaria-programme

/reports/world-malaria-report-2024), states that 597,000 individuals died of malaria in 2023 (World malaria report 2023, 2023). Although anemia is a major cause of death due to hemolysis and dyserythropoiesis (White, 2018; White, 2022), multiple organ failure (MOF) and resultant sepsis syndrome are also important, particularly in severe, acute infections (World malaria report 2023, 2023). Ongoing global warming

E-mail address: mmizu@med.nagoya-u.ac.jp (M. Mizuno).

<sup>\*</sup> This article is part of a Special issue entitled: 'Complement System During Infectious Disease' published in Immunobiology.

<sup>\*</sup> Corresponding author at: Department of Renal Replacement Therapy, Nagoya University Graduate School of Medicine, 65 Tsurumai-cho, Showa-ku, Nagoya, Japan.

will expand the at-risk malaria endemic areas and will likely increase the number of malarial patients. Numerous effective antimalarial agents are now clinically available and development of new antimalarial agents and vaccines is progressing; nevertheless, the burden of death remains, in part because current therapies are administered too late to prevent progression to MOF (World malaria report 2023, 2023). Lethality in malaria-infected individuals is usually because of severe anemia due to hemolysis and dyserythropoiesis (White, 2018; White, 2022), multiple organ failure (MOF), including renal, liver and neurological impairment and resultant sepsis syndrome (World malaria report 2023, 2023; Yashima et al., 2017; Ohno et al., 2019; Hora et al., 2016). To explore the pathological mechanisms underpinning these effects of malarial parasites, several mouse models mimicking cerebral malaria, sepsis, lung injury, renal failure and MOF have been developed, most involving infection with P. berghei (Yashima et al., 2017; Hunt et al., 2010; Koide et al., 2012; Ortolan et al., 2014; Zuzarte-Luis et al., 2014; Das, 2008).

Complement (C), an important immune defense system in blood, has the capacity to induce self-injuries caused by excessive activation, hence is often referred to as a "double-edged sword" (Mizuno and Morgan, 2004; Mizuno et al., 2018). The relationship between malaria and C has attracted discussion with both protective and harmful roles proposed for the human host (Biryukov and Stoute, 2014; Ohno et al., 2019). It is well known that C dysregulation can drive damage in diverse organs; for example, we have demonstrated abundant C3 activation in a rat membranoproliferative glomerulonephritis model (Yashima et al., 2017). In a mouse model of cerebral malaria, C5 deficiency, but not C5a receptor deficiency, was demonstrated to be protective, implicating the terminal pathway and membrane attack complex (MAC, C5b-9) (Ramos et al., 2011). However, the roles of C terminal pathway in other organ injuries in malaria remain unexplored.

In the present study, we investigated roles of the terminal pathway in a mouse malaria model initiated by infection with *P. berghei* NK65 (PbNK65). We chose to use C6-deficient mice to test the role of terminal pathway/MAC assembly as cleavage of C5 to C5b and C5a generation is maintained in these mice. The data demonstrate a strong protective effect of C6 deficiency, implicating MAC and informing new approaches to therapy in human malaria.

#### 2. Materials and methods

#### 2.1. Animals

C6 deficient (C6def) mice were backcrossed to C57BL/6J mice for more than 10 generations and their genetic background was identical to that of C57BL/6J mice (Ten et al., 2010). Wild-type (WT) C57BL/6J mice of the same age were purchased from Charles River Japan, Inc. (Yokohama, Japan) for use as controls in infection experiments. Sevenweek-old WT and C6def male mice were used with an initial body weight of 22-27 g. To harvest control blood samples, we also used 7 agematched, uninfected WT and C6def mice. The mice were fed a commercial CE-2 diet (CREA Japan, Tokyo, Japan) and had ad libitum access to water; they were housed in a pathogen-free facility at the Institute for Laboratory Animal Research, Graduate School of Medicine, Nagoya University, and maintained under controlled conditions (temperature 23  $\pm$  1 °C, humidity 55  $\pm$  10 %, light cycle 12 h light/12 h dark). Experiments involving parasite infection in mice were performed in an ABSL2 (Animal Bio-Safety Level 2) animal facility at the Institute. All experimental procedures were performed under isoflurane inhalation anesthesia. Animal care and all experimental procedures were approved by the Animal Care and Use Committee, Graduate School of Medicine, Nagoya University, and were conducted according to the Nagoya University Regulations on Animal Care and Use in Research.

#### 2.2. Agents and antibodies

Sodium heparin was purchased from Mochida pharmaceutical Co.

(Tokyo, Japan). For immunohistochemistry analysis, fluorescein isothiocyanate (FITC) -labeled polyclonal (pc) goat anti-C3 antibody was purchased from MP Biomedicals (Santa Ana, CA), FITC-labeled pc rabbit (Rb) anti-human fibrinogen was from DAKO (Santa Clara, CA). Pc Rb anti-rat C9 antibody which cross-reacted with mouse C9/MAC was made in-house according to past report (Mizuno et al., 1997; Mizuno et al., 2009; Morgan et al., 2006). Rat monoclonal Ab (mAb) anti-mouse CD45 (clone 30-F11) was purchased from eBioscience<sup>TM</sup> (SanDiego, CA). Secondary antibodies, Alexa Fluor® 488-labeled donkey anti-rat IgG and FITC-labeled goat anti-rabbit IgG were purchased from Jackson ImmunoResearch (West Grove, PA). Before incubation with secondary antibodies, sections were blocked with 10 % ( $\nu/\nu$ ) Blocking One (Nacalai Tesque, Kyoto, Japan).

#### 2.3. Infection with malarial parasites in mice

Mouse erythrocytes infected with the rodent malaria parasite *Plasmodium (P.) berghei* NK65 (PbNK65) were stored as frozen stock at  $-80\,^{\circ}\text{C}$  until use. These were freshly thawed and passaged once in WT male mice, parasitized erythrocytes harvested and injected intraperitoneally (i.p.;  $1\times10^6$  per mouse) into seven-week old male C6def and WT mice.

To evaluate malarial parasite infection, blood samples were harvested from tail vessels, the blood smeared on a glass slide (FF-011, Matsunami Glass Ind., Osaka, Japan), fixed with methanol (FUJIFILM Wako, Osaka, Japan) for 5 min at room temperature and air-dried.

Blood smears on glass slides were stained with May Grunwald-Giemza stain (May-Grunwald staining stock solution and Giemza stock solution, Merck Millipore, Darmstadt, Germany), examined under light microscopy (LM) with x400 magnification, and total and parasite-infected erythrocytes were counted over ten fields to calculate % PbNK65 infection.

# 2.4. In Vivo experimental protocols and evaluation of microscopic findings in organs

First, we investigated whether absence of the terminal pathway influenced survival of mice infected systemically with the PbNK65 malarial parasite by comparing C6def and WT mice ( $n=11,\ n=8,$  respectively) by following for 26 days after i.p. injection of  $1\times 10^6$  parasitized erythrocytes. Pathological changes in liver, lung, kidney, heart and brain were assessed at day 7 in selected mice to clarify the focus and severity of organ injuries.

Macroscopic and microscopic evidence of tissue injury was found in liver and lung but not other organs at day 7; a separate study thus focused on liver, lung and blood changes on day 7 after PbNK65 infection in C6def (n=12) and WT (n=16; one died prior to day 7 so excluded from analysis) mice. Body weight was measured daily and behavior twice daily; infection with PbNK65 was confirmed on day 6 after i.p. inoculation using tail-bleed whole blood smear samples stained with May Grunwald-Giemza as above.

#### 2.5. Preparation of blood and tissue samples

For evaluation of parasite-infected erythrocyte number and measures of blood analysis and blood chemistry, blood was harvested from tail vein at intervals during the observation period and at sacrifice by cardiac puncture, collected in 5 U/ml of sodium heparin.

Tissues were harvested, coded and randomly separated for blinded LM analysis, IF analysis and mRNA evaluations.

### 2.6. Histological and immunofluorescence (IF) analysis

Harvested tissues were randomly dissected into four blocks ( $\sim 5 \times 5$  mm, from each tissue). For LM analysis, two blocks were fixed in 10 % ( $\nu/\nu$ ) buffered formalin, and embedded in paraffin wax. Sections were

cut (3  $\mu$ m) and stained with periodic acid-Schiff (PAS) for kidney and hematoxylin and eosin (HE) for other tissues. To evaluate accumulation of neutrophils, the Fast Blue Salt esterase reaction method was used (Iguchi et al., 2018). Briefly, deparaffinized sections were incubated in chloroacetate solution (comprising 5 mg naphthol AS-D chloroacetate dissolved in 1 ml of  $N_i$ 0-dimethylformamide mixed with 25 mg fast blue BB salt and diluted in 40 ml of PBS), for 60 min at room temperature in the dark. After rinsing, nuclei were counterstained with Nuclear Fast Red counterstain (Vector Laboratories, Burlingame, CA).

For IF analysis, the other two blocks were snap-freeze embedded in Tissue-Tec<sup>TM</sup> O.C.T. Cryomold (Sakura Finetek Japan, Tokyo, Japan) with Surgipath FSC 22 Clear frozen section compound (Leica biosystems, Nussloch, Germany) and frozen sections (3 µm) prepared. To evaluate deposition of fibrinogen and C3b, frozen sections were incubated with FITC-labeled anti-fibrinogen and FITC-labeled anti-C3 antibodies, respectively. To observe deposition of C5b-9, sections were incubated with anti-C9 antibody followed by FITC-labeled anti-Rb IgG. To count CD45-positive white blood cells, sections were stained with anti-CD45, followed by incubation with Alexa488-labeled anti-rat IgG.

## 2.7. Evaluation of pathological changes and degree of complement deposition

Inflammatory cell accumulation in liver and lung was assessed by IF, counting number of CD45-positive cells and esterase-positive neutrophils in five fields under x400 magnification; the average was used for each animal

Liver tissue damage was defined as accumulation of inflammatory cells, necrotic changes, occlusion of sinusoid, and/or vacuolation of hepatocytes in tissues. These parameters were evaluated in whole-block sections from each animal (2 blocks per animal) by LM at  $\times$ 400 magnification. Severity of liver tissue injuries was scored for each section using the scale: 0, no change; 1, minimal change (accumulation of inflammatory cells, less than 25 %/field); 2, mild injury (accumulation of inflammatory cells between 25 and 65 %/field without necrotic changes); 3, moderate injury (accumulation of inflammatory cells was observed less than 65 %/field without necrotic changes); 4, severe injury (necrotic changes with accumulation of inflammatory cells in less than 50 %/fields); 5, very severe injury (necrotic changes with accumulation of inflammatory cells in <50 %/fields).

To evaluate deposition of fibrinogen, C3b and C5b-9 sections were viewed in six fields under x400 magnification and scored for each parameter as: 0, negative to minimum (less than 5 %/field); 1, mild (between 5 and 33 %/field); 2, moderate (between 33 and 67 %/field); 3, severe (more than 67 %/field). The mean of five fields was calculated for each animal.

### 2.8. Blood cell counts and biochemistry

After collection of blood, Blood Cell Count (white blood cells (WBC), hemoglobin (Hb), and platelet (Plt)) was immediately measured on a pocH  $^{\rm TM}$ -100iV automated analyzer (Sysmex Corporation, Kobe, Japan). The remaining blood sample was centrifuged at 2000 rpm for 10 min, plasma harvested and stored at  $-80\,^{\circ}{\rm C}$  until use. Plasma albumin (Alb), alanine transaminase (ALT), aspartate transaminase (AST), and alkaline phosphatase (ALP) were measured on an automated analyzer at a contract research facility (Sanritz Serkova Inspection Center Nagoya Laboratory, Nagoya, Japan).

#### 2.9. ELISA for complement activation and inflammation markers

To investigate plasma levels of the C activation products C3a and C5a, TECO® Mouse C3a ELISA (TECK Medical Group, Sissach, Switzerland) and C5a Mouse ELISA Kit (Abcam, Eugene, OR) were used as instructed by manufacturers. IL-6, a prototypic inflammatory cytokine, was measured using Mouse IL-6 ELISA kit (R&D systems,

Minneapolis, MN). ELISA plates were read using a Multiskan Sky plate reader (Thermo Fisher Scientific, Waltham, MA).

### 2.10. Quantitative Real-Time PCR (qRT-PCR) assessment of C3 expression in tissues

To investigate expression of mRNA in liver and lung, harvested tissues were immediately placed in RNA stabilization solution (RNA later™ soln; Thermo Fisher Scientific, Waltham, MA) on ice, incubated at 4  $^{\circ}\text{C}$  overnight, then stored at -80  $^{\circ}\text{C}$  until use. Tissues were homogenized and total RNA extracted using RNeasy Mini Kit (QIAGEN, Venlo, Nederland), isolated total RNA adjusted to a concentration of 500 ng, then reverse transcribed to complementary DNA (cDNA) using the High-Capacity cDNA Reverse Transcription Kit (Thermo Fisher Scientific), following manufacturers information. The purified cDNA was stored at -80 °C. PCR primers specific for mouse C3 (Mm01232779 m1) were used to amplify C3 cDNA. All primers were made by Taqman Gene Expression (Thermo Fisher Scientific, Waltham, MA). For real-time quantitative (RT-q) PCR, stored cDNA, RNA free water, primers, and Tagman Fast MasterMix were mixed; amounts of each mRNA were calculated and compared by the  $\Delta\Delta$ CT method using Step One plus (Thermo Fisher Scientific), with 18SrRNA (Thermo Fisher Scientific) as the endogenous control as in our previous report (Tomita et al., 2017).

#### 2.11. Statistical analysis

Time-to-death was compared using Kaplan-Meier survival curves. For analysis of pathological changes under LM, log-rank tests were performed. Non-parametric analyses for comparison among multiple groups were performed by the Kruskal-Wallis test and comparisons between two groups were performed by the Mann-Whitney U test. Values of p < 0.05 were considered statistically significant. GraphPad Prism 9.0 (Graphpad Software Inc., La Jolla, CA, USA) was used for statistical analysis. Values are shown as mean  $\pm$  standard deviation.

### 3. Results

# 3.1. C6 deficiency significantly reduces weight loss and prolongs survival of mice infected with PbNK65

Survival of WT mice infected with PbNK65 parasites was only 50 % on day 7 and all mice died within 10 days after the infection. In contrast, survival of PbNK65 parasite-infected C6def mice was 100 % on day 7 and more than 80 % on day 10 post-infection (Fig. 1A). After day 20, survival in the infected C6def mice fell rapidly with 100 % dead by day 26 (Fig. 1A), suggesting a second, delayed mode of death in the absence of C6.

Mice were weighed daily up to day 7 post-infection; although both WT and C6def mice lost weight, the degree of weight loss was significantly greater in WT mice (18.6 % weight loss between day 0 and day 6 in WT compared to 13.1 % loss in C6def mice; Fig. 1B). To evaluate proliferation of PbNK65 parasites on day 6, the percentage of parasite-infected erythrocytes were measured; percentage infection on day 6 was not significantly different between C6def and WT mice (Fig. 1C).

### 3.2. C6 deficiency protects from early organ injury and inflammatory cell accumulation in mice infected with PbNK65

Because most WT mice died within 8 days after PbNK65 infection, organ injury in PbNK65-infected C6def and WT mice was assessed at day 7 (Fig. 2). In WT mice, PbNK65 infection caused severe liver injuries with hyaline-like deposition, necrosis and degradation of hepatocytes (Fig. 2C). Although most C6def mice showed some liver injury at this timepoint compared to uninfected WT (Fig. 2A, E), scores were significantly lower than those in WT mice (Fig. 2G). Lung injuries were assessed by LM at day 7 post-infection, measuring alveolar hemorrhages,

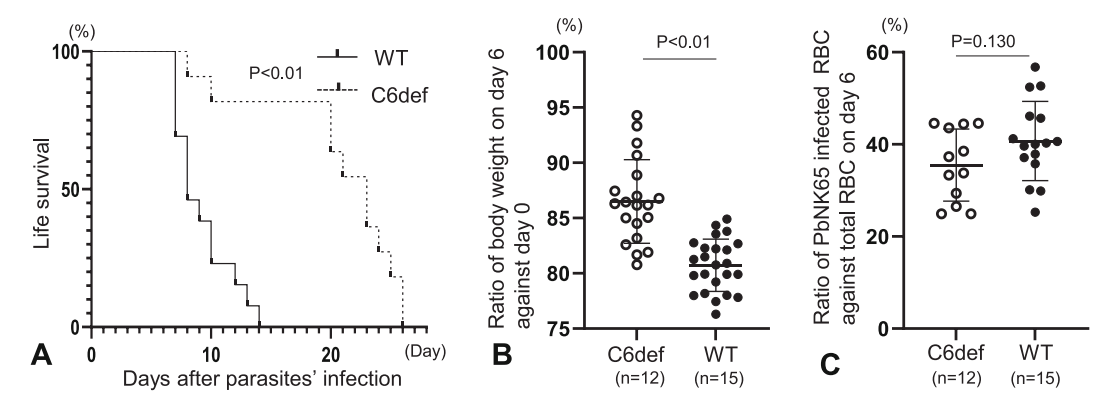


Fig. 1. Impact of C6 deficiency on parasite load, weight loss and survival after infection with Plasmodium (P.) berghei NK65 (PbNK65) parasites. Wild-type (WT) and C6 deficient (C6def) mice were injected with  $1 \times 10^6$  red blood cells (RBC) infected with PbNK65 parasites. A. Survival, presented as Kaplan Meier curves was markedly increased in C6def (dotted line) compared to WT (solid line) mice. B. Both strains showed decreased body weight on day 6 post-infection compared to pre-infection (day 0) but this was significantly greater in WT ( $\sim$ 20 %) compared to C6def ( $\sim$ 13 %). C. Parasite load, assessed by measuring proportion of infected RBCs, was not significantly different between C6def and WT mice at day 6. P < 0.05 was considered significant.

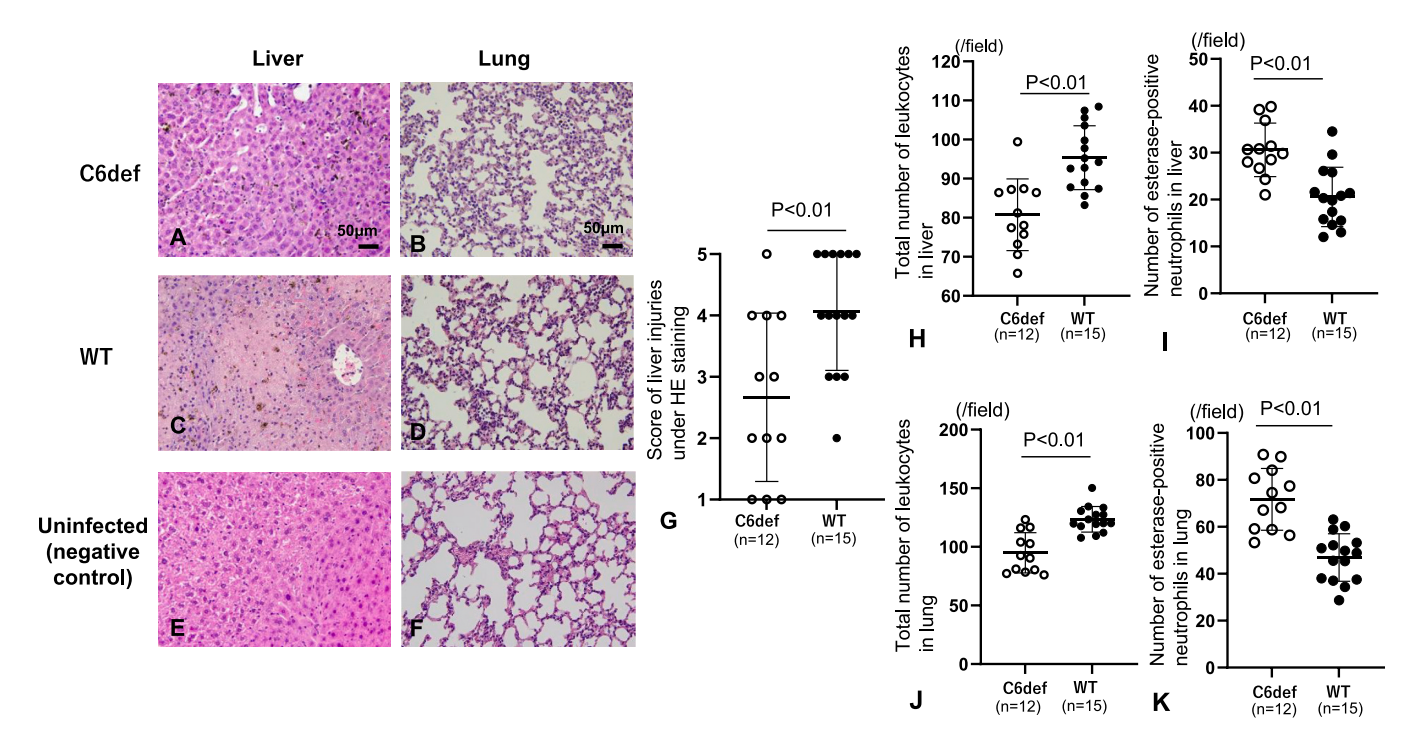


Fig. 2. Microscopic changes in liver and lung of C6def and WT mice on day 7 after infection with *Plasmodium (P.) berghei* NK65 (PbNK65) parasites. In liver (A, C, E) tissue injury, assessed in H-E sections as described in Methods, was apparent in both mouse strains post-infection compared to uninfected controls but was significantly greater in WT compared to C6def (G), demonstrating protection from injury in absence of MAC. In lung (B, D, F) tissue injury assessed as described was minimal post-infection, not different from uninfected controls.

Graphs H and J show total white blood cell (leukocyte) counts in liver and lung respectively, demonstrating significantly higher leukocyte accumulation in WT compared to C6def mice in both organs. Graphs I and K show counts of esterase-positive neutrophils in liver and lung respectively, demonstrating significantly higher neutrophil infiltration in C6def compared to WT mice in both organs.

Original magnification x400. Scale bars were shown in right-lower corners of frames A and B. P < 0.05 was considered significant.

fibrin deposition and eosinophilic hyaline deposition as seen in the acute exudative phase of acute respiratory distress syndrome (ARDS) (Matthay et al., 2019). However, lung injures were mild and accumulation of inflammatory cells was only observed in WT and C6def mice and not significantly different between the groups on day 7 (Fig. 2B, D, and F).

To investigate inflammatory cell accumulation in liver and lung on day 7 post-infection with PbNK65, total WBC count and esterase-positive neutrophil count were measured in both C6def and WT mice. Total WBC counts were markedly elevated in WT mice at 7 days post-infection in liver and lung; in comparison, WBC counts were significantly lower in both organs in C6def mice (Fig. 2H and J). Surprisingly,

neutrophil counts showed the opposite, significantly higher in C6def compared to WT mice at 7 days post-infection in lung and liver.

Tissue injuries in heart, brain, kidney and spleen at day 7 post-infection were also measured in and compared between C6def and WT mice; no significant pathological changes were observed in these tissues in either mouse line (Fig. 3).

3.3. C6 deficiency reduces complement and fibrinogen deposition in organs in PbNK65-infected mice

In WT and C6def mice at 7 days post-infection with PbNK65, there

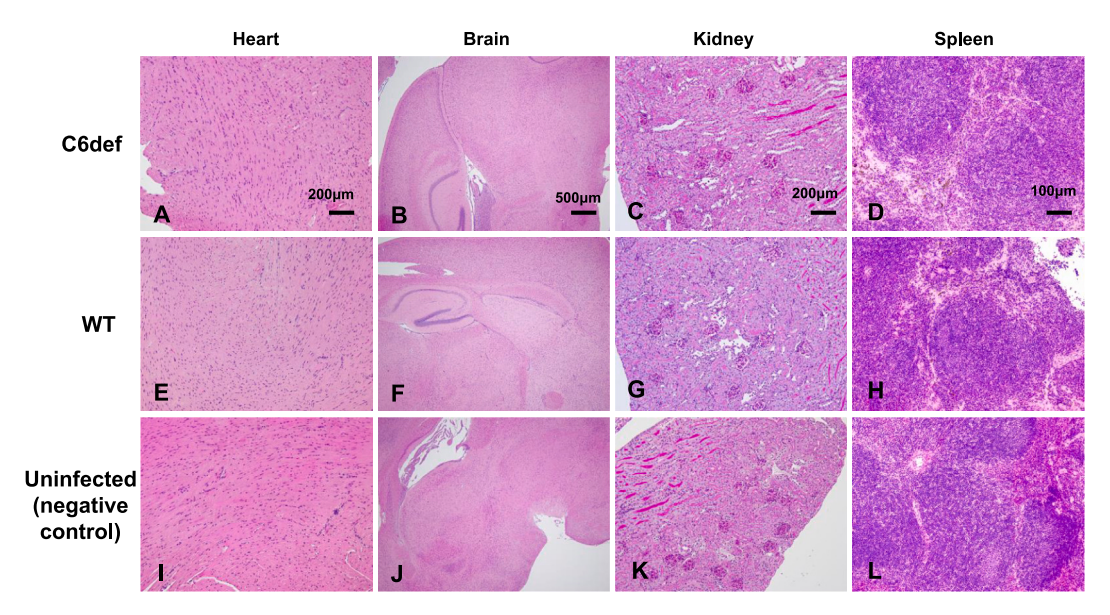


Fig. 3. Microscopic findings in heart, brain, kidney and spleen of C6 deficient (C6def) and wild type (WT) mice on day 7 after PbNK65 infection. Tissue injury was assessed in H-E sections from heart (A, E, I; x100 as original magnification), brain (B, F, J; x40), kidney (C, G, K; x100) and spleen (D, H, L; x400) in uninfected mice (I – L) and at day 7 post-infection in C6def (A – D) and WT (E – H) mice. No obvious tissue injury was observed in these organs at 7 days post-infection compared to uninfected. Scale bar is shown in right-lower corners of frames A to D.

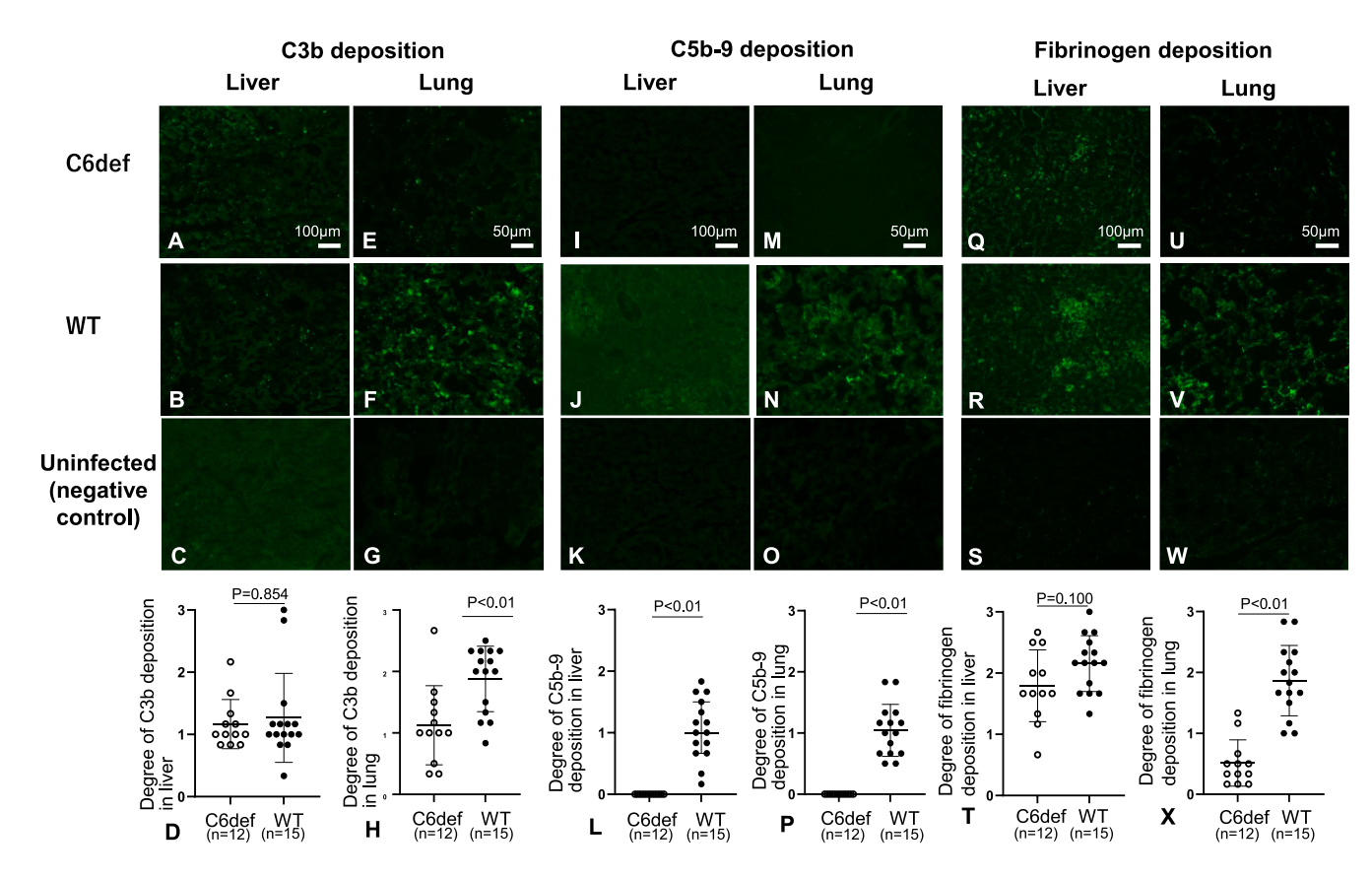


Fig. 4. Depositions of C3b, C5b-9 and fibrinogen in liver and lung of C6def and WT mice on day 7 after PbNK65 infection. Deposition of C3b was assessed in liver (A - C) and U (E - G) of uninfected mice (C, G) and C6def (A, E) and WT (B, F) mice at 7 days post-infection. C3b deposition in liver was not different between C6def and WT mice (D); however, in lung, C3b deposition was significantly reduced in C6def compared to WT (H). Deposition of C5b-9 was assessed in liver (I - K) and lung (M - O) of uninfected mice (K, O) and C6def (I, M) and WT (J, N) mice 7 days post-infection. In C6def mice, C5b-9 staining was absent in both liver and lung as expected while C5b-9 staining was high in both organs in WT mice at day 7 post-infection (L, P). Deposition of fibrinogen was assessed in liver (Q - S) and lung (U - W) of uninfected mice (S, W) and C6def (Q, U) and WT (R, V) mice 7 days post-infection. Fibrinogen deposition in liver was not different between C6def and WT mice (T); however, in lung, fibrinogen deposition was significantly reduced in C6def compared to WT (X).

Original magnification for liver sections was x200 and for lung sections was ×400. Scale bars are shown in right-lower corner of frames A, E, I, M, Q and U.

was abundant C3b deposition in liver compared to controls (Fig. 4A-C) but no significant difference between WT and C6def (Fig. 4D). In lung, C3b deposition was increased in both groups but was significantly higher in WT compared to C6def (Fig. 4E-H) Deposition of C5b-9 was abundant in liver and lung of WT mice on day 7 after PbNK65 infection (Fig. 4J and N), while no staining for C5b-9 was seen in either organ from C6def mice (Fig. 4I and M), confirming absence of terminal pathway in the absence of C6. Neither C3b nor C5b-9 deposition was observed in the liver or lung of uninfected mice, confirming the specificity of the staining (Fig. 4 C, G, K and O).

In WT mice at 7 days post-infection with PbNK65, there was abundant fibrinogen deposition in both lung and liver (Fig. 4R and V). In comparison, in lung tissues of C6def mice post-infection, deposition of fibrinogen was significantly lower than in WT mice (Fig. 4U, V and X). Although deposition of fibrinogen in liver of C6def mice with parasite infection was lower than in infected WT mice, the difference was not significant (Fig. 4T).

# 3.4. C6 deficiency ameliorated platelet loss and liver injury in PbNK65-infected mice

Blood WBC counts were significantly increased on day 7 post-PbNK65 infection in both C6def and WT mice compared to uninfected controls, but were not significantly different between the groups (Fig. 5A). Blood Hb levels were markedly decreased post-infection in both C6def and WT mice compared with uninfected controls, demonstrating the severity of the infection-induced anemia; however, levels were not significantly different between C6def and WT mice (Fig. 5B). Blood Plt counts were markedly reduced post-infection in WT mice but not in C6def mice compared to uninfected controls (Fig. 5C).

A set of plasma analytes, Alb, AST, and ALT, associated with general condition and liver function, were measured in C6def and WT mice on day 7 post-PbNK65 infection. Plasma levels of Alb were significantly decreased post-infection in both C6def and WT mice; comparison between the groups demonstrated a significantly smaller decrease in C6def mice (Fig. 5D). Plasma levels of AST and ALT, indicators of liver injury, were significantly increased post-infection in both C6def and WT mice compared with uninfected controls but were not different between the groups (Fig. 5E and F).

### 3.5. Plasma levels of IL-6 and C5a, but not C3a are elevated post-infection

Plasma levels of IL-6, a prototypic inflammatory cytokine, were elevated in 7 day post-infection plasma; levels in C6def mice were significantly lower than in WT mice (Fig. 6A). Plasma levels of C5a, but not C3a, were elevated post-infection in both groups and not significantly different between the groups (Fig. 6B and C).

To evaluate whether infection with PbNK65 parasites influenced C3 production in liver, expression of C3 mRNA in liver was measured at day 7. Expression of C3 mRNA was up-regulated in both C6def and WT mice post-infection compared with the uninfected groups but was not significantly different between C6def and WT mice (Fig. 6D).

#### 4. Discussion

Activation of C is a critical component of the initial host protection against invaders such as microorganism and parasites (Biryukov and Stoute, 2014; Mizuno et al., 2018); however, C activation can drive inflammation and tissue damage to the host that causes pathology, seen

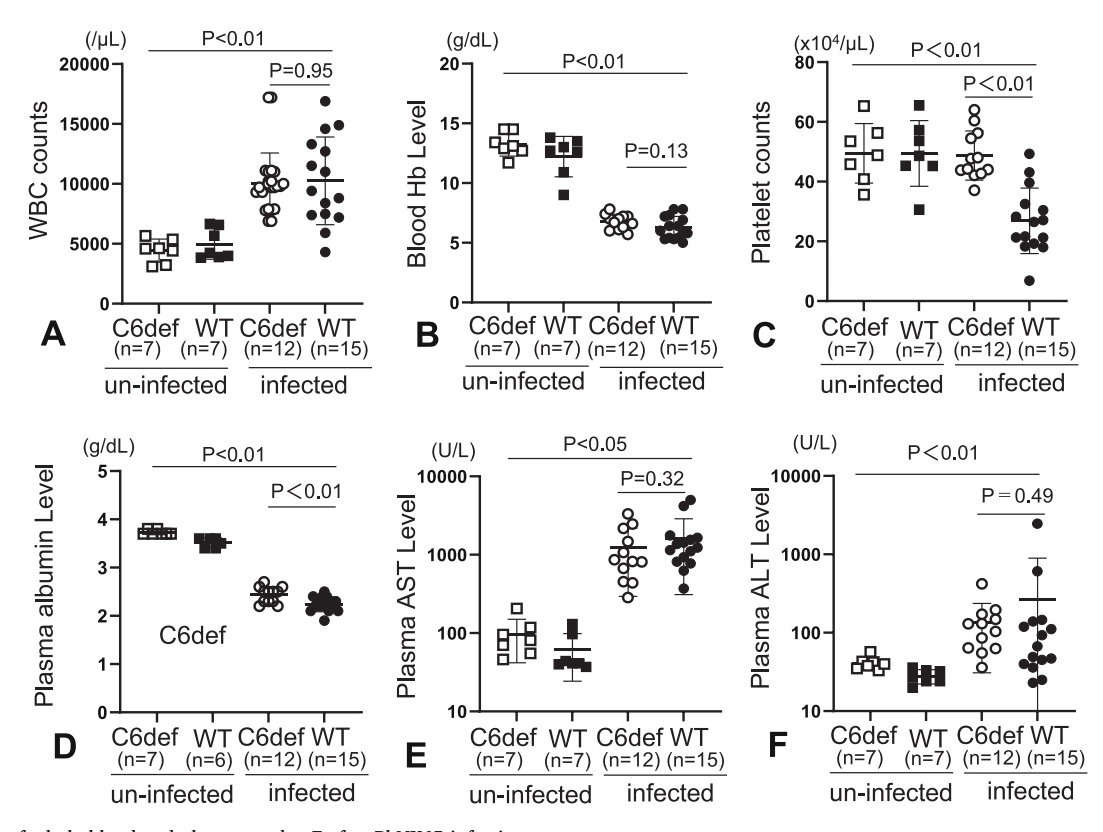


Fig. 5. Analysis of whole blood and plasma on day 7 after PbNK65 infection.

White blood cell counts (WBC) (A), blood hemoglobin (Hb) levels (B), platelets (Plt) count (C), plasma albumin (Alb) levels (D), plasma alanine aminotransferase (ALT) levels (E), and plasma aspartate aminotransferase (AST) levels (F) were measured in C6def and WT mice, either uninfected or at day 6 post-infection with PbNK65 parasites. WBC, AST and ALT increased post-infection in both mouse strains, while Hb levels, platelet counts and plasma albumin levels decreased post-infection. Platelet counts were markedly reduced post-infection in WT mice but were significantly higher and comparable to uninfected in C6def mice (C). Plasma albumin levels were also significantly lower in WT compared to C6def mice post-infection (D). P < 0.05 was considered significant.

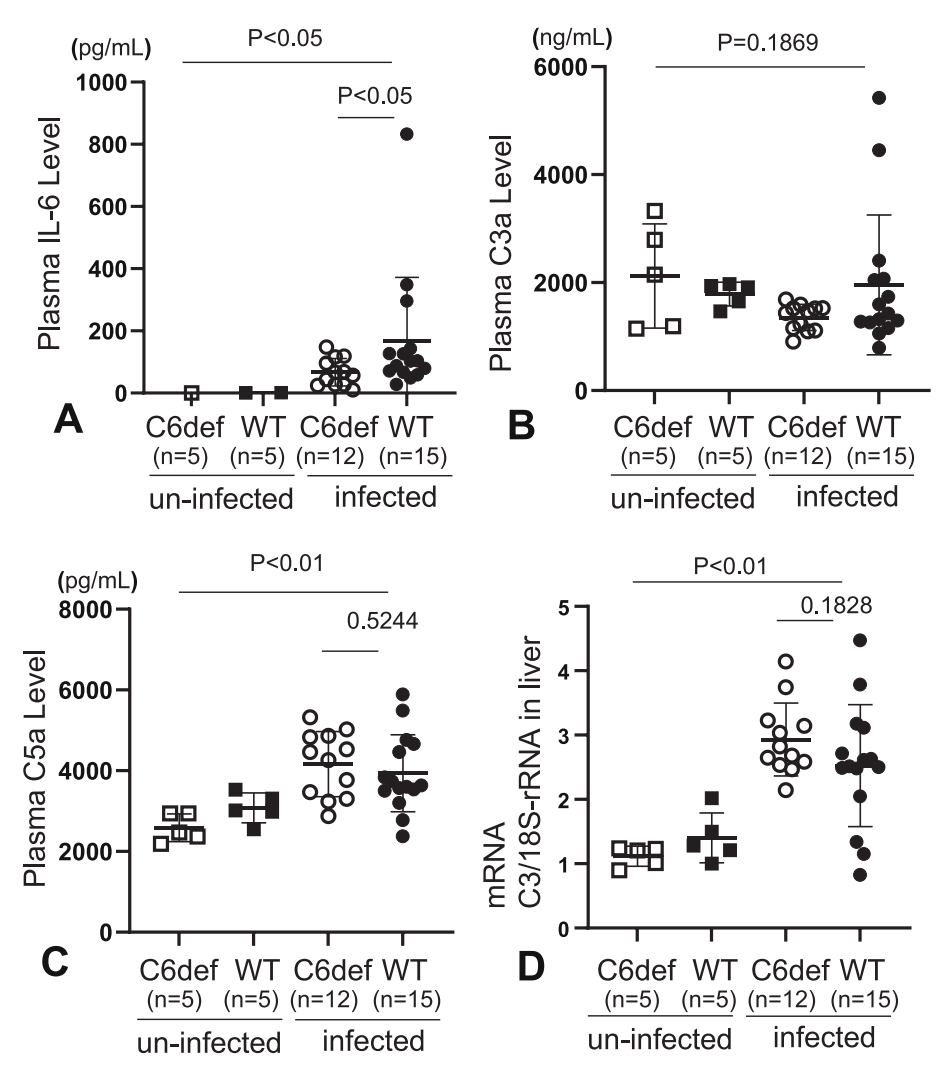


Fig. 6. Plasma levels of interleukin-6 (IL-6), C3a and C5a, and hepatic expression of C3 in C6def and WT mice on day 7 after PbNK65 infection. Plasma levels of IL-6 were up-regulated in both C6def and WT mice after PbNK65 infection and were significantly higher in WT compared to C6def mice post-infection (A). Plasma C3a levels were not significantly different between uninfected and infected mice of either strain (B). Plasma levels of C5a were significantly increased in both C6def and WT mice after PbNK65 infection, but were not significantly different between the strains (C). C3 message expression in liver was significantly increased post-infection in C6def and WT mice but was not different between the strains post-infection (E). P < 0.05 was considered significant.

in diverse diseases (Mizuno et al., 2018; Mizuno and Morgan, 2011). In malaria, although it has been reported that the C system can play both protective and harmful roles in the host (Biryukov and Stoute, 2014), a detailed understanding of roles of C, and particularly the relevance of the TP and MAC assembly, remain unclear. C5 deficiency was reported to prevent lethal cerebral malaria in a mouse model, suggesting that activation of the TP and generation of C5a and/or MAC might be a critical driver of cerebral malaria (Ramos et al., 2011). The impact on systemic pathologies and differentiation of C5a and MAC effects remain unexplored. Here we set out to fill this knowledge gap by testing the impact of deficiency of C6, an essential component for MAC assembly, on the course of disease in a mouse malaria model.

WT mice infected with PbNK65 malarial parasites developed anemia and MOF dominated by severe liver and lung injures, pneumonia and thrombocytopenia with over half of the infected mice dying within 8 days post-infection and 100 % by day 14. In contrast, C6def mice were strongly protected with 80 % surviving at day 20. In WT mice, death was likely a direct consequence of the severe liver injuries, lung inflammation and severe thrombocytopenia, all of which were markedly attenuated in C6def mice at day 7 post-infection, firmly implicating TP activation and MAC formation in these fatal sequelae of infection. Notably, neither blood proliferation of the parasites nor infection-

induced severe anemia were impacted by C6 deficiency, but there were no significant difference in parasite load or blood Hb levels between C6def and WT mice at day 7 post-infection, indicating that the TP did not significantly regulate parasite proliferation, likely a consequence of their protected location.

Deposition of C activation products C3b and C5b-9 was abundant in lung and liver, of parasite-infected WT mice, demonstrating local C dysregulation; in C6def mice C5b-9 staining was absent, confirming absence of terminal pathway activity, while C3b deposition was markedly attenuated. Notably, plasma levels of C5a were elevated post-infection but were not different between infected WT and C6def mice. Hepatic expression of C3, a known marker of the acute phase, was also increased post-infection to the same extent in both WT and C6def mice, demonstrating that hepatic production of C3, the source of plasma C3, was not impacted by C6 deficiency. In contrast, levels of IL6, the main cytokine driver of the acute phase, were elevated in WT compared with C6def mice post-infection, indicating that C6 deficiency reduced systemic inflammation induced by malarial infection in the model.

Interestingly, accumulation of neutrophils in lung and liver was higher in C6def mice compared in WT mice, and was less than in C6def mice in contrast with the reduced degree of tissue injuries in the absence of C6. We suggest that the continued production of the neutrophil

chemotaxins C3a and C5a, unaffected by C6 deficiency, drive the observed neutrophil accumulation while the absence of C6, by blocking MAC formation, reduces tissue damage. Comparison of C6def and C5def mice in the model would help address this anomaly as a future study.

Taken together, the results demonstrate that C activation, and specifically TP activation and MAC formation, drive the development of MOF, anemia and thrombocytopenia that cause acute death in mice infected with PbNK65 parasites in this malaria model. Critically, C6 deficiency delayed rather than prevented death in the model; although most infected C6def mice survived beyond day 21, they then rapidly declined with all dying by day 28. Parasite load continued to increase over this period and anemia progressed (supplementary Fig. 1), suggesting that the C6def mice eventually succumb because of TPindependent severe and progressive anemia due to parasite burden, a well-described and critical factor in malarial deaths (White, 2018; White, 2022). Nevertheless, absence of TP activity markedly delayed death. Given that numerous drugs targeting C5 are already available, and others targeting C6 or C7 are in development, repurposing to prevent these acute consequences of malarial infection is feasible. As we show, such interventions will likely not prevent parasite proliferation and its consequences; however, early TP inhibition, by preventing MOF and other acute events, may open a therapeutic window to enable the effective use of anti-malarial therapies that prevent pathogen proliferation and clear the infection. Further proof of concept by testing terminal pathway blocking drugs in combination with other interventions in malaria models is now needed to test this possibility.

Supplementary data to this article can be found online at https://doi. org/10.1016/j.imbio.2025.153140.

#### **Authors statement**

We are not aware of any information that would constitute a conflict of interest in this study and do not wish specifically to exclude potential reviewers. All authors have contributed for this manuscript and stated in the manuscript. This manuscript has been read and approved for submission by all authors, and is not under review elsewhere.

Masashi Mizuno, on behalf of all authors.

#### **Funding**

This work was supported in part by the Ministry of Education, Culture, Sports, Science and Technology in Japan Grants-in-Aid 18K08206, 21K08274, 21K08275, and 22K08309 for Scientific Research. BPM is supported by the UK Dementia Research Institute which receives its funding from UK DRI Ltd., funded by the UK Medical Research Council, Alzheimer's Society and Alzheimer's Research UK.

#### Declaration of generative AI

None.

#### Declaration of competing interest

The authors declare the following financial interests/personal relationships which may be considered as potential competing interests: Masashi Mizuno reports was provided by Nagoya University Graduate School of Medicine. If there are other authors, they declare that they have no known competing financial interests or personal relationships that could have appeared to influence the work reported in this paper.

#### Acknowledgements

Authors thank N. Suzuki, N. Asano, and Y. Sawa for technical support. M. Mizuno, Y. Suzuki, H. Kim, H. Kojima, and S. Fukui worked in the Department of Renal Replacement Therapy in positions endowed by Vantive Japan at Nagoya University Graduate School of Medicine.

#### Data availability

Data will be made available on request.

#### References

- Biryukov, S., Stoute, J.A., 2014. Complement activation in malaria: friend or foe? Trends Mol. Med. 20, 293–301. https://www.sciencedirect.com/science/article/pii/S1471 491414000021
- Das, B.S., 2008. Renal failure in malaria. J. Vector Borne Dis. 45, 83–97. http://www.mrcindia.org/journal/issues/452083.pdf.
- Hora, R., Kapoor, P., Thind, K.K., Mishra, P.C., 2016. Cerebral malaria-clinical manifestations and pathogenesis. Metab. Brain Dis. 31, 225–237. https://doi.org/ 10.1007/s11011-015-9787-5.
- Hunt, N.H., Grau, G.E., Engwerda, C., Barnum, S.R., van der Heyde, H., Hansen, D.S., Schofield, L., Golenser, J., 2010. Murine cerebral malaria: the whole story. Trends Parasitol. 26, 272–274. https://www.sciencedirect.com/science/article/pii/ \$1471492210000590
- Iguchi, D., Mizuno, M., Suzuki, Y., Sakata, Y., Maruyama, Y., Okada, A., Okada, H., Ito, Y., 2018. Anti-C5a complementary peptide mitigates zymosan-induced severe peritonitis with fibrotic encapsulation in rat pretreated with methylglyoxal. Am. J. Physiol. Ren. Physiol. 315, F1732–F1746. https://doi.org/10.1152/ aiprenal.00172.2018.
- Koide, N., Morikawa, A., Odkhuu, E., Haque, A., Badamtseren, B., Naiki, Y., Komatsu, T., Yoshida, T., Yokochi, T., 2012. Low susceptibility of NC/Nga mice to the lipopolysaccharide-mediated lethality with D-galactosamine sensitization and the involvement of fewer natural killer T cells. Innate Immun. 18, 35–43. https://doi.org/10.1177/1753425910390400.
- Matthay, M.A., Zemans, R.L., Zimmerman, G.A., Arabi, Y.M., Beitler, J.R., Mercat, A., Herridge, M., Randolph, A.G., Calfee, C.S., 2019. Acute respiratory distress syndrome. Nat. Rev. Dis. Primers 5, 18. https://www.nature.com/articles/s41572-0 19-0069-0
- Mizuno, M., Morgan, B.P., 2004. The possibilities and pitfalls for anti-complement therapies in inflammatory diseases. Curr. Drug. Targets. Inflamm. 3, 87–96. https://www.eurekaselect.com/article/36403.
- Mizuno, M., Morgan, B.P., 2011. An update on the roles of the complement system in autoimmune diseases and the therapeutic possibilities of anti-complement agents. Curr. Drug Ther. 6, 35–50. https://www.eurekaselect.com/article/18024.
- Mizuno, M., Nishikawa, K., Goodfellow, R.M., Piddlesden, S.J., Morgan, B.P., Matsuo, S., 1997. The effects of functional suppression of a membrane-bound complement regulatory protein, CD59, in the synovial tissue in rats. Arthritis Rheum. 40, 527–533. https://doi.org/10.1002/art.1780400319.
- Mizuno, M., Ito, Y., Hepburn, N., Mizuno, T., Noda, Y., Yuzawa, Y., Harris, C.L., Morgan, B.P., Matsuo, S., 2009. Zymosan, but not lipopolysaccharide, triggers severe and progressive peritoneal injury accompanied by complement activation in a rat peritonitis model. J. Immunol. 183, 1403–1412. https://journals.aai.org/jimm unol/article/183/2/1403/82423.
- Mizuno, M., Suzuki, Y., Ito, Y., 2018. Complement regulation and kidney diseases: recent knowledge of the double-edged roles of complement activation in nephrology. Clin. Exp. Nephrol. 22, 3–14. https://doi.org/10.1007/s10157-017-1405-x.
- Morgan, B.P., Chamberlain-Banoub, J., Neal, J.W., Song, W., Mizuno, M., Harris, C.L., 2006. The membrane attack pathway of complement drives pathology in passively induced experimental autoimmune myasthenia gravis in mice. Clin. Exp. Immunol. 146, 294–302.
- Ohno, T., Miyasaka, Y., Kuga, M., Ushida, K., Matsushia, M., Kawabe, T., Kikkawa, Y., Mizuno, M., Takahashi, M., 2019. Mouse NC/Jic strain provides novel insights into host genetic factors for malaria research (NC mouse as a new mode for malaria). Exp. Anim. 68, 243–255. https://www.sciencedirect.com/science/article/pii/S1471491414000021.
- Ortolan, L.S., Sercundes, M.K., Barboza, R., Debone, D., Murillo, O., Hagen, S.C., Russo, M., Lima, M.R.D. Império, Alvarez, J.M., Amaku, M., Marinho, C.R., Epiphanio, S., 2014. Predictive criteria to study the pathogenesis of malariaassociated ALI/ARDS in mice. Mediat. Inflamm. 2014, 872464. https://doi.org/ 10.1155/2014/872464.
- Ramos, T.N., Darley, M.M., Hu, X., Billker, O., Rayner, J.C., Ahras, M., Wohler, J.E., Barnum, S.R., 2011. Cutting edge: the membrane attack complex of complement is required for the development of murine experimental cerebral malaria. J. Immunol. 186, 6657–6660. https://academic.oup.com/jimmunol/article/186/12/6657/ 7006802
- Ten, V.S., Yao, J., Ratner, V., Sosunov, S., Fraser, D.A., Botto, M., Sivasankar, B., Morgan, B.P., Silverstein, S., Stark, R., Polin, R., Vannucci, S.J., Pinsky, D., Starkov, A.A., 2010. Complement component c1q mediates mitochondria-driven oxidative stress in neonatal hypoxic-ischemic brain injury. J. Neurosci. 30, 2077–2087. https://www.jneurosci.org/content/30/6/2077.
- Tomita, T., Arai, S., Kitada, K., Mizuno, M., Suzuki, Y., Sakata, F., Nakano, D., Hiramoto, E., Takei, Y., Maruyama, S., Nishiyama, A., Matsuo, S., Miyazaki, T., Ito, Y., 2017. Apoptosis inhibitor of macrophage ameliorates fungus-induced peritoneal injury model in mice. Sci. Rep. 7, 6450. https://www.nature.com/articles/sal1598-017-06824-6
- White, N.J., 2018. Anaemia and malaria. Malar. J. 17, 371. https://doi.org/10.1186/ s12936-018-2509-9.
- White, N.J., 2022. Severe malaria. Malar. J. 21, 284. https://doi.org/10.1186/s12936-022-04301-8.

- World malaria report 2023, 2023. Geneva2023 Contract No.: Licence: CC BY-NC-SA 3.0 IGO. https://www.who.int/teams/global-malaria-programme/reports/world-malaria-report-2023 (accessed 13 May 2025).
- Yashima, A., Mizuno, M., Yuzawa, Y., Shimada, K., Suzuki, N., Tawada, H., Sato, W., Tsuboi, N., Maruyama, S., Ito, Y., Matsuo, S., Ohno, T., 2017. Mesangial proliferative glomerulonephritis in murine malaria parasite, Plasmodium chabaudi AS, infected
- NC mice. Clin. Exp. Nephrol. 21, 589–596. https://doi.org/10.1007/s10157-016-
- Zuzarte-Luis, V., Mota, M.M., Vigário, A.M., 2014. Malaria infections: what and how can mice teach us. J. Immunol. Methods 410, 113–122. https://www.sciencedirect.com/science/article/pii/S0022175914001318.